Journal of Alzheimer's Disease 54 (2016) 585–595
DOI 10.3233/JAD-160067
IOS Press

The Association Between Retinal Neuronal Layer and Brain Structure is Disrupted in Patients with Cognitive Impairment and Alzheimer's Disease

Siwei Liu[a,1], Yi-Ting Ong[b,1], Saima Hilal[d,e], Yng Miin Loke[a], Tien Y. Wong[b], Christopher Li-Hsian Chen[d,e], Carol Y. Cheung[b,f,2] and Juan Zhou[a,c,2,*]
[a]*Center for Cognitive Neuroscience, Neuroscience and Behavioral Disorders Program, Duke-National University of Singapore Medical School, Singapore*
[b]*Singapore Eye Research Institute, Singapore National Eye Centre, Singapore*
[c]*Clinical Imaging Research Centre, The Agency for Science, Technology and Research and National University of Singapore, Singapore*
[d]*Department of Pharmacology, National University of Singapore, Singapore*
[e]*Memory Aging & Cognition Centre, National University Health System, Singapore*
[f]*Department of Ophthalmology and Visual Sciences, The Chinese University of Hong Kong, Hong Kong*

Accepted 9 June 2016

Abstract. Both healthy and pathological aging due to Alzheimer's disease (AD) are associated with decreased brain grey matter volume (GMV) and disrupted white matter (WM) microstructure. Thinner macular ganglion cell-inner plexiform layer (GC-IPL) measured by spectral-domain optical coherence tomography has been reported in patients with AD and mild cognitive impairment. Emerging evidence suggested a link between thinner GC-IPL and lower GMV in subjects with no dementia using region-of-interest-based approach. However, it remains unknown whether GC-IPL thickness is associated with brain WM microstructure and how such association differed between normal and cognitively impaired subjects. Here, for subjects with no cognitive impairment (NCI), thinner GC-IPL was associated with lower WM microstructure integrity in the superior longitudinal fasciculus, inferior fronto-occipital fasciculus, corticospinal tracts, anterior thalamic radiation, and cingulum regions, while it was weakly associated with lower GMV in visual cortex and cerebellum. Nevertheless, these retina-brain associations were disrupted in the presence of cognitive impairment. Correlations between GMV and GC-IPL were lost in patients with cognitive impairment but no dementia (CIND) and AD patients. GC-IPL was related to WM microstructural disruption in similar regions with decreased significance. In contrast, lower WM microstructure integrity in the fornix showed a trend of correlation with thinner GC-IPL in both CIND and AD but not NCI. Collectively, our findings suggest the possible physiological retina-brain relationship in healthy aging, which might be disrupted by disease-induced changes in patients with cognitive impairment. Longitudinal study with larger patient sample should follow to confirm the disease mechanism behind these retina-brain relationship changes.

Keywords: Alzheimer disease, diffusion tensor imaging, mild cognitive impairment, optical coherence tomography, retinal ganglion cells, white matter

[1]Joint first authors.

[2]Joint senior authors.

*Correspondence to: Juan Zhou, PhD, Duke-NUS Medical School, 8 College Road, #06-15, Singapore 169857, Singapore. Tel.: +65 66012392; Fax: +65 62218685; E-mail: helen.zhou@duke-nus.edu.sg.

INTRODUCTION

While normal aging is usually accompanied with loss of grey matter volume (GMV) in the brain, accelerated brain atrophy is associated with pathological aging such as Alzheimer's disease (AD). Structural magnetic resonance imaging (MRI) is a traditional region-of-interest quantification approach that is often focused on the temporal regions affected by normal aging and more profoundly by AD [1–3]. The whole-brain voxel-based morphometry (VBM) method can provide a whole-brain spatially non-biased evaluation of AD-related grey matter (GM) atrophy as well as enhanced spatial specificity [4–7]. In parallel, diffusion tensor imaging (DTI) measures of white matter (WM) microstructure are useful in measuring healthy and pathological aging [8, 9]. Fractional anisotropy (FA), a commonly reported diffusivity measure of WM microstructure, indexes the directional coherence of water displacement. Previous literature revealed region-specific WM microstructural disruption in AD and mild cognitive impairment (MCI), commonly represented as reduced FA, including commissural, association, and limbic fiber tracts, whereas projection fiber tracts were relatively preserved until advanced stages of the disease [10–21].

Furthermore, emerging evidence demonstrated a possible link between reduction of peripapillary retinal nerve fiber layer (RNFL) thickness as measured by optical coherence tomography (OCT) with AD [22]. With the newer spectral-domain OCT, it further showed that macular ganglion cell-inner plexiform layer (GC-IPL) thinning was more strongly associated with MCI, compared with periperpillary RNFL thinning [23]. A recent study also found a close association between GC-IPL thinning and smaller GMV of the occipital and temporal lobes in elderly subjects [24], suggesting that macular GC-IPL might be a better indictor to access neurodegenerative processes than peripapillary RNFL axonal reduction. However, this study divided the whole-brain into five regions only (including frontal, parietal, occipital, temporal, and central regions) to examine the relationship between GMV and retinal neuronal damage. Whole-brain voxel-wise analyses are needed to address region-specific GMV damage associated with OCT arrays.

Importantly, it remains unknown if GC-IPL thickness in the retina is related to WM microstructure in the brain. Particularly, differential region-specific WM microstructural changes might be associated with GC-IPL loss in subjects with different severity of cognitive impairment. Here, using whole-brain voxel-wise approach (for both GM and WM), we sought to test whether GC-IPL thinning was associated with brain GMV reductions and WM microstructural changes [lower FA and higher mean diffusivity (MD)] and how such association differed between normal and cognitively impaired subjects (patients with cognitive impairment but no dementia (CIND) and AD, respectively). This study may corroborate the associations between regions-specific brain structure (both GM and WM) and GC-IPL, improve our understanding of the physiological variations, and aid in the differentiation between physiological and pathological structural changes related to AD.

METHODS

Participants

Participants with subjective complaints of memory problems and/or demonstrated cognitive impairment on neuropsychological assessment were recruited from two study sites in Singapore, i.e., memory clinics from National University Hospital and St. Luke's Hospital. Control subjects with no cognitive impairment (NCI) on neuropsychological assessment were recruited from both memory clinic and the community [25]. All subjects were administered the Mini-Mental State Examination, the Montreal Cognitive Assessment, Clinical Dementia Rating, Geriatric Depression Scale, the informant questionnaire on cognitive decline, and a formal neuropsychological battery locally validated for older Singaporeans (see details in our previous work [26]) by trained psychologists. Ethics approval was obtained from National Healthcare Group Domain-Specific Review Board (DSRB). The study was conducted in accordance with the Declaration of Helsinki. Written informed consent was obtained, in the preferred language of the participants, by bilingual study coordinators.

We grouped our participants based on objective measurements of cognitive impairments, which is an extensive assessment validated previously for Singaporean elderly [27]. This neuropsychological test battery examines seven domains including executive function, attention, language, visuomotor speed, visuoconstruction, verbal memory, and visual memory [26, 27]. Diagnoses of cognitive impairment and dementia were made at weekly consensus meetings reviewing clinical history, blood investigations,

neuropsychological assessment, and neuroimaging data. The diagnosis of CIND was determined by clinical judgment and was defined as, no loss of independence in daily activities, and impairment in at least one domain of the neuropsychological test battery. Participants were considered to have failed a test if they scored 1.5 SD below the education-adjusted cut-off values of each test [28]. Failure in at least half of the tests in each domain was considered as impairment in that domain. Dementia was diagnosed in accordance with DSM-IV criteria. The etiological diagnoses of AD were made according to National Institute of Neurological and Communicative Disorders and Stroke and the Alzheimer's Disease and Related Disorders Association (NINCDS-ADRDA) guidelines. For the NCI, we ensured that participants have no impairment in any of the seven domains in the extensive neuropsychological tests [24, 26, 27].

All participants were excluded from this study if they were/had: (1) Hypoxic/anoxic, hypotensive, hypertensive, uremic or hepatic encephalopathy; (2) Traumatic, nutritional, or toxic disorder affecting the central nervous system (CNS); (3) Current substance abuse disorder (e.g., alcohol, barbiturates, opiates, amphetamines, phencyclidine, or cocaine as defined by the DSM-IV) or past substance use disorder affecting the CNS; (4) Intracerebral hemorrhage that could cause cognitive impairment; (5) Cranial arteritis, CNS inflammatory vasculitides, Moyamoya disease; (6) CNS infection including syphilis, tuberculosis, fungi, rickettsiae, bacterium, viral encephalitis, Creutzfield-Jacob disease, or other CNS infection; (7) Space occupying intracranial mass lesion; (8) Obstructive or normal pressure hydrocephalus; (9) Difficult to control epilepsy that could cause cognitive impairment; and (10) patients with schizophrenia or bipolar disorder. Subjects with vascular CIND or vascular dementia were also excluded if one or more of the following conditions existed: (1) Medical illness requiring concomitant corticosteroid or immunosuppressant therapy; (2) Moribund state (mRS >4); (3) Significant aphasia/dysarthria that significantly impedes cognitive assessment (NIHSS Best language (Aphasia) and Dysarthria score >1); (4) Pacemakers or other metallic implants which were not compatible with 3T MRI. Out of 191 participants included in this study, only 4 participants had Geriatric Depression Scale scores higher than 9 (1 NCI and 3 CIND) and 11 took antidepressants, anxiolytics, and/or antipsychotics medications (2 NCI, 4 CIND, and 5 AD; among these 11 participants, good GC-IPL thickness measurements were available for 1 NCI, 2 CIND, and 4 AD).

Subjects were also assessed for neuroimaging evidence of significant cerebrovascular disease. To minimize the potential confounding influence of cerebrovascular disease, subjects with the presence of any of the following: (1) cortical infarcts; (2) two or more lacunes; (3) confluent WM lesions in two regions of the brain (Age Related WM Changes scale score $\geq$8) [29] were excluded from the analysis [25].

Out of 411 eligible participants recruited between August 12, 2010 to August 21, 2014, 10 participants had no MRI scans, 164 participants had MRI evidence of cerebrovascular disease, and 46 participants did not pass quality control for both DTI and MRI data. Among the remaining 191 participants, 2 participants (NCI) did not pass the structural MRI quality control, while the other 11 participants (4 NCI and 7 CIND) were excluded due to motion artifacts in DTI data (details in Methods). Therefore, we studied the group difference in WM microstructure in 65 NCI, 68 CIND, and 47 AD and the WM-GC-IPL association in a subset of 124 subjects who passed the retina imaging quality control (WM cohort, Table 1). We studied the GMV group differences and the associations with GC-IPL in a slightly different cohort (GMV cohort, Supplementary Methods and Supplementary Table 1). Subject demographics were comparable between the WM and GMV samples. There was no significant group difference in gender and handedness. There was no significant difference in age between NCI and CIND, while AD patients were older than both groups. Ethnicity in CIND was significantly different from NCI. In all analyses, we included age, gender, handedness, and ethnicity as covariates.

Retinal imaging and processing

After pupil dilation using tropicamide 1% and phenylephrine hydrochloride 2.5%, Cirrus HD-OCT (Carl Zeiss Meditec) was used to acquire macular and optic disc scans using macular cube 200 $\times$ 200 and optic nerve head cube 200 $\times$ 200 scan protocols respectively in each eye from each subject. In brief, GC-IPL thickness was detected and measured from an elliptical annulus area (14.13 mm^2) centered on the fovea with an inner vertical diameter of 1 mm, an outer vertical diameter of 4 mm, an inner horizontal diameter of 1.2 mm and an outer horizontal diameter of 4.8 mm. A series of GC-IPL parameters (average, superior, superonasal, inferonasal, inferior,

Table 1
Subject demographic, neuropsychological, and GC-IPL thickness features

Group	NCI	CIND	AD	F or χ^2, df, p
N (for WM cohort)	65	68	47	
Age Years	67.3 (6.2)[a]	69.7 (8.2)[a]	75.2 (7.8)[n,c]	15.72, (2,177), <0.001
Gender M:F	29 : 36	35 : 33	17 : 30	2.63, 2, 0.27
Handedness R:L	60 : 5	65 : 3	47 : 0	3.80, 2, 0.22
Ethnicity C:M:I:Mx:O	60 : 2:3 : 0:0[c]	55 : 2:11 : 0:0[n]	38 : 6:1 : 1:1	20.52, 8, 0.009
MMSE	27.4 (2.0)[c,a]	25.2 (3.3)[n,a]	16.6 (5.2)[n,c]	135.6, (2,177), <0.001
CDR	0.1 (0.2)[c,a]	0.3 (0.2)[n,a]	1.1 (0.3)[n,c]	225.6, (2,177), <0.001
N (with GC-IPL thickness)	47	50	27	
GC-IPL Thickness	80.19[c] (5.89)	76.92[n] (6.29)	78.41 (5.85)	3.73, (2, 114), 0.03

The values N represent the number of subjects in the white matter (WM) analysis cohort as well as its subset with retina measures used in this study. Superscript letters indicate whether group mean was significantly different from NCI (n), CIND (c), and AD (a), based on *post hoc* pairwise comparisons ($p < 0.05$). Within a subgroup of participants who had gradable OCT, group comparisons of GC-IPL thickness were done controlling for age, gender, handedness and ethnicity. NCI, no cognitive impairment; CIND, cognitive impairment without dementia; AD, Alzheimer's disease; MMSE, Mini-Mental State Evaluation; CDR, Clinical Dementia Rating scale; GM, grey matter; WM, white matter; df, degree of freedom; M:F, male:female; R:L, right:left, C:M:I:Mx:O, Chinese:Malay:Indian:Mix:Others.

inferotemporal, superotemporal sectors) were derived by automated segmentation algorithm available on the Cirrus HD-OCT which delineates the outer boundaries of the ganglion cell layer and inner plexiform layer. Cirrus HD-OCT optic disc scan protocols have also been described in our previous work [23]. A trained grader masked to subject characteristics inspected all macular cube scans for image quality. We excluded scans with glaucoma history and retinal pathology affecting GC-IPL thickness measurement (such as epiretinal membrane, macula edema, vitreomacular traction, age-related macular degeneration, etc.). Scans with GC-IPL algorithm segmentation failure, probably due to poor scan signal strength or quality, were also excluded from our analysis. According to these criteria, a total of 56 subjects were excluded from analysis (Table 1 and Supplementary Table 1).

Neuroimaging data acquisition

DTI scans were obtained using 32-channel head coil on a 3T Siemens Tim Trio system (Erlangen, Germany) at Clinical Imaging Research Center, National University of Singapore, using a diffusion-weighted echo-planar imaging sequence (61 non-collinear diffusion gradient directions at $b = 1150\ s/mm^2$, seven volumes of $b = 0\ s/mm^2$, TR/TE = 6800/85 ms, FOV = $256 \times 256\ mm^2$, matrix = 84×84, 48 contiguous slices, and slice thickness = 3.0 mm). High-resolution T1-weighted structural MRI was acquired using MPRAGE (magnetization-prepared rapid gradient echo) sequence (192 continuous sagittal slices, TR/TE/TI = 2300/1.9/900 ms, flip angle = 9°, FOV = $256 \times 256\ mm^2$, matrix = 256×256, isotropic voxel size = $1.0 \times 1.0 \times 1.0\ mm^3$, bandwidth = 240 Hz/pixel).

White matter microstructure derivation

The DTI data were preprocessed using FSL v5.0 (http://www.fmrib.ox.ac.uk/fsl; [30] following our previous approach [31]. Eddy current distortion and head movement [32] were corrected through affine registration of diffusion-weighted images to the first b = 0 volume. Brain Extraction Tool (BET) was used for brain extraction and creating a brain mask with fractional intensity threshold of 0.25. Maximum motion was calculated within this brain mask for each subject by taking the maximum displacement of volumes from the first b = 0 volume [33]. Participants with more than 3 mm maximum motion were excluded from further analysis. Diffusion gradients were rotated to improve consistency with the motion parameters. Individual's maps were visually inspected for signal dropout, artifacts, and additional motion. FA and MD images were created by fitting a diffusion tensor model to the diffusion data at each voxel (DTIFIT, FSL). We then applied Tract-Based Spatial Statistics (TBSS) [34] to analyze the FA data in the major brain WM tracts. FA images were first non-linearly registered [35] and transformed to the high resolution ($1\ mm^3$) FMRIB58_FA image. The FA images were skeletonized and represented the center of the major WM tracts in the brain. The MD images were created similarly to the FA images.

Voxel-based morphometry

We applied an optimized voxel-based morphometry (VBM8) [36] using Statistical Parametric Mapping (SPM8) (http://www.fil.ion.ucl.ac.uk/spm/). We

derived the subject-level GMV probability maps from T1 structural images following our previous approach [35, 36], including: (1) segmented individual T1-weighed images into GM, WM, and cerebrospinal fluid; (2) created a study-specific template using non-linear DARTEL registration [37]; (3) registered each GM/WM probability maps to the customized template in MNI space and performed tissue segmentation; (4) performed modulation by multiplying voxel values by the Jacobian determinants derived from the spatial normalization step; (5) applied smoothing on the normalized GM maps by a 10 mm isotropic Gaussian kernel. Individual GMV maps were normalized (divided by total estimated intracranial volume) for further statistical analyses.

Statistical analyses

Group comparisons

To examine the pair-wise group difference in WM FA and MD, we built voxel-wise general linear models (GLM) with the skeletonized WM FA or MD images as the dependent variable, group as the covariate of interest, and age, gender, handedness, and ethnicity as the nuisance variables. The WM regions where the skeletonized FA and MD were significantly different between the three groups were identified using permutation-based non-parametric testing (FSL RANDOMISE), thresholded at $p < 0.005$ with threshold-free cluster enhancement (TFCE) and family-wise error (FWE) correction and with minimum cluster size of 100 voxels [38]. Anatomical localization of the identified WM clusters was determined with reference to the Johns Hopkins University white matter atlas (20 labels) [39].

Similar voxel-wise GLM was built with the subject-level normalized GMV probabilistic maps as dependent variable. Significant group differences in GMV were identified using two-sample *t*-tests (SPM8), thresholded at FWE corrected $p < 0.05$.

Correlation between brain structure measures and GC-IPL thickness

To examine the association between GC-IPL thickness with WM FA and MD, we built voxel-wise GLM with the skeletonized WM FA or MD images as the dependent variable, GC-IPL thickness as the covariate of interest, and OCT signal strength, age, gender, handedness, and ethnicity as the nuisance variables. The WM regions where the skeletonized FA were positively correlated GC-IPL were identified using permutation-based non-parametric testing (FSL RANDOMISE), thresholded at $p < 0.05$ with TFCE and FWE correction [38], with minimum cluster size of 100 voxels. We repeated the same analyses to test the negative correlation between the skeletonized MD and GC-IPL thickness. Analyses of correlations between WM FA/MD and GC-IPL thickness were conducted both across participant groups and within each participant group.

We built the same voxel-wise GLM to examine the association between GMV and GC-IPL thickness both within each group and across all three groups (SPM8), thresholded at voxel-wise uncorrected $p < 0.001$ and cluster size larger than 500 voxels.

RESULTS

Retina imaging characteristics

Within those participants with OCT scans of sufficient quality for analysis, GC-IPL was significantly thinner in CIND than in NCI [$F(1, 90) = 7.367$, $p = 0.008$]. No difference in GC-IPL was observed in AD compared to the other two groups (Table 1).

Group difference in WM microstructure and GMV

We observed that lower WM microstructure integrity (evidenced by lower FA and higher MD, FWE corrected $p < 0.005$) in CIND and AD compared to NCI (Supplementary Figure 1, Supplementary Table 2). Compared to the NCI group, FA in frontal (bilateral anterior thalamic radiation (ATR), bilateral corticospinal tracts (CST), forceps minor, bilateral uncinate fasciculus), temporal-parietal (forceps major), temporal-occipital (right inferior longitudinal fasciculus), temporal (right temporal part of superior longitudinal fasciculus), frontal-occipital/parietal (bilateral inferior fronto-occipital fasciculus (IFO) and bilateral superior longitudinal fasciculus (SLF)), and cingulum (bilateral cingulum cingulate gyrus (CG)) brain regions were lower in the CIND group. MD was significantly larger in frontal (bilateral ATR, forceps minor, bilateral uncinate fasciculus, and bilateral CST), frontal-occipital/parietal (bilateral IFO and SLF), and cingulum (left CG) brain regions. Further lower WM microstructural integrity was found in the AD patients compared to the CIND patients. While those regions damaged in CIND worsen in AD, damages also extended to bilateral cingulum hippocampus,

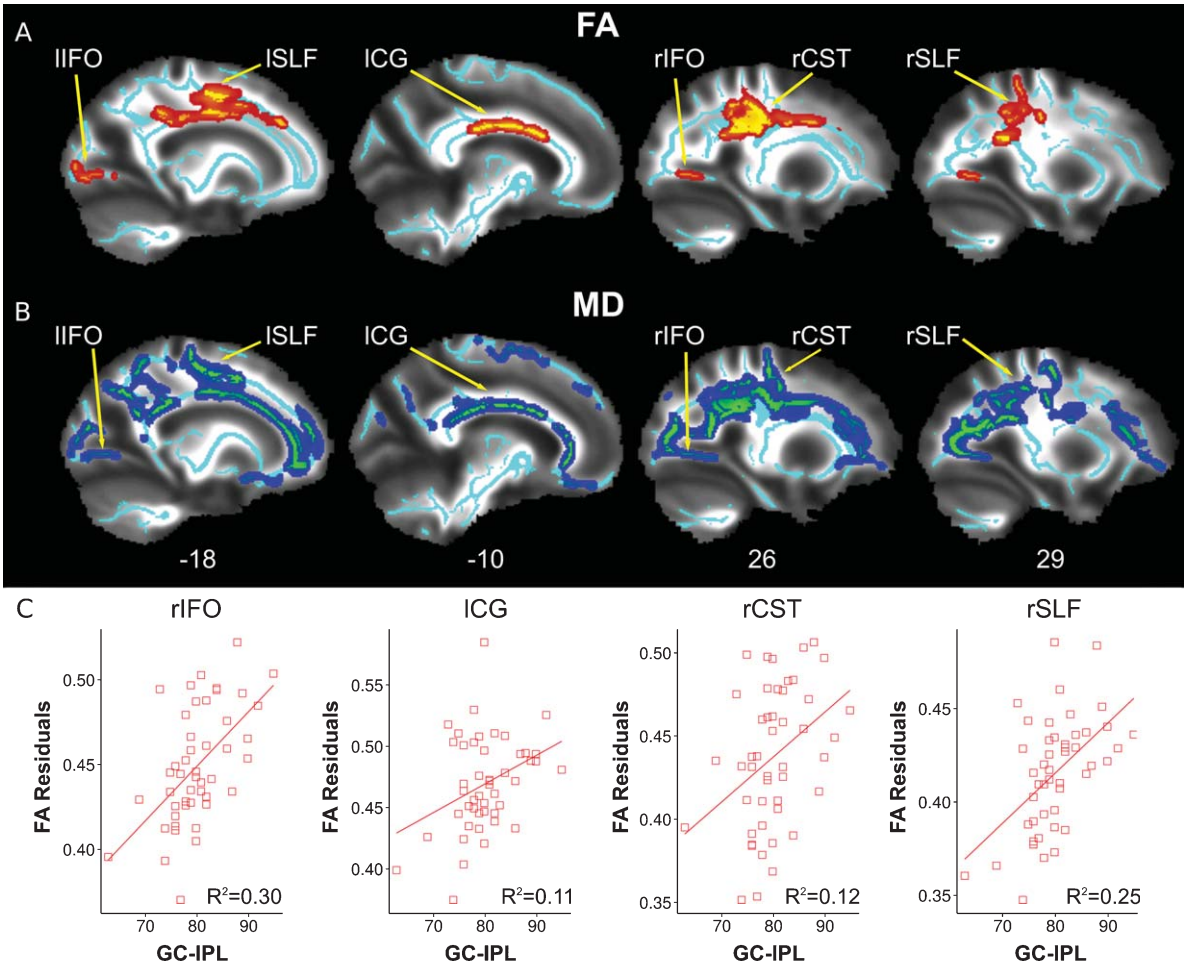

Fig. 1. Correlation of GC-IPL thickness with white matter microstructure in the NCI group. The group-level skeletonized mean FA (cyan color) was thresholded to reflect major WM tracts in the brain [34]. Voxel-wise Linear Regression based on TBSS revealed (A) significant positive correlation of GC-IPL thickness with FA in brain regions highlighted in red-yellow and (B) significant negative correlation between GC-IPL thickness and MD in brain regions highlighted in blue-green colours (FWE corrected $p < 0.05$). C) The subject-level mean FA values from four clusters (pointed by the yellow arrows in A) were plotted against the GC-IPL thickness for the NCI group (red squares and red solid line) after regressing out the effects of SD-OCT scanner signal strength, age, gender, handedness, and ethnicity. Adjusted R^2 was reported for each cluster. NCI, no cognitive impairment; GC-IPL, ganglion cell-inner plexiform layer; WM, white matter; FA, fractional anisotropy; MD, mean diffusivity; TBSS, tract-based spatial statistics; FWE, family-wise error; SD-OCT, spectral domain optical coherence tomography; rIFO, right inferior fronto-occipital fasciculus; lIFO, left inferior fronto-occipital fasciculus; lCG, left cingulum cingulate gyrus; rCST, right corticospinal tract; rSLF, right superior longitudinal fasciculus; lSLF, left superior longitudinal fasciculus.

bilateral inferior longitudinal fasciculus, and bilateral CG for FA.

We observed lower GMV in CIND and AD compared to NCI (Supplementary Figure 2 and Supplementary Table 3). Compared to the NCI group, GMV in temporal, frontal, and occipital regions were significantly smaller in the AD group (voxel-wise FWE $p < 0.05$). At the same threshold of voxel-wise FWE corrected $p < 0.05$, lower GMV was found in frontal regions in the AD compared to the CIND group, while there was no significant difference between the CIND and the NCI groups.

Thinner GC-IPL is related to lower WM microstructural integrity

In NCI, we found that lower FA and higher MD values were significantly associated with GC-IPL thinning in frontal (bilateral ATR and forceps minor), parietal (bilateral CST), frontal-occipital/parietal (bilateral IFO and bilateral SLF), and cingulum (bilateral CG) (FWE corrected $p < 0.05$, Fig. 1, Supplementary Table 4).

Under the same threshold (FWE corrected $p < 0.05$), we did not find significant correlations

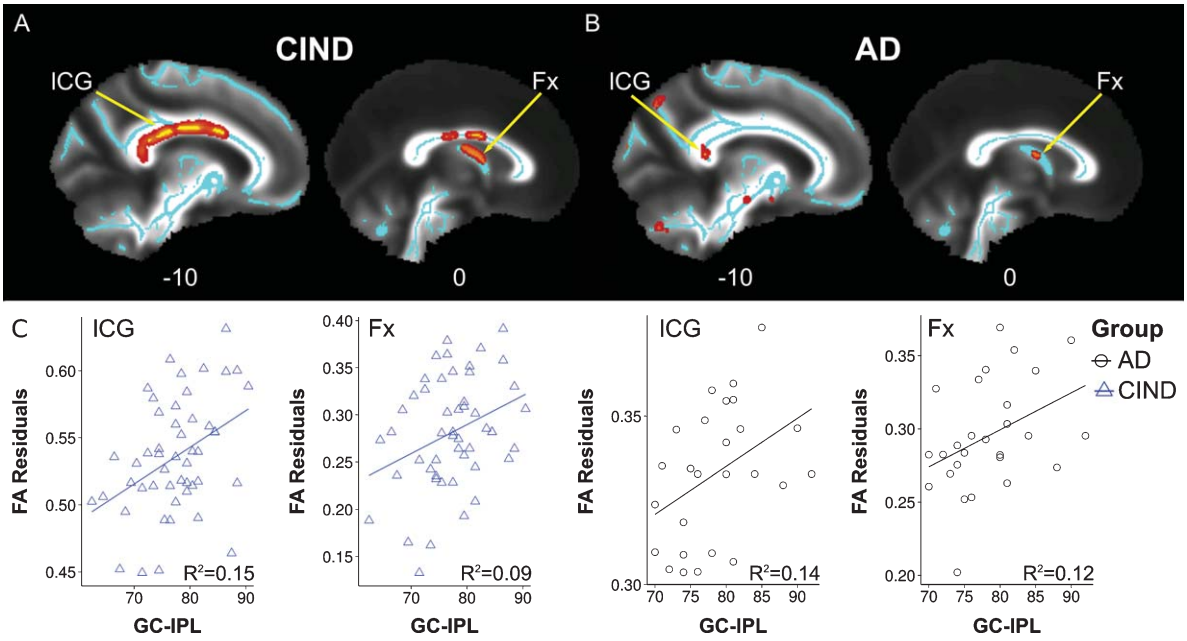

Fig. 2. Correlation of GC-IPL thickness with white matter FA in the CIND and the AD groups. The group-level skeletonized mean FA (cyan color) was thresholded to reflect major WM tracts in the brain [34]. Voxel-wise Linear Regression based on TBSS revealed positive correlation trend of GC-IPL thickness with FA in left CG and fornix (pointed by the yellow arrows in A and B) highlighted in red-yellow colors (TFCE uncorrected $p < 0.05$) in both the CIND (A) and the AD (B) groups. C) The subject-level mean FA values from these two clusters were plotted against the GC-IPL thickness (blue triangles and blue solid line for the CIND; black circles and black broken line for the AD), after regressing out the effects of SD-OCT scanner signal strength, age, gender, handedness, and ethnicity. Adjusted R^2 was reported for each cluster. CIND, cognitive impairment without dementia; AD, Alzheimer's disease; GC-IPL, ganglion cell-inner plexiform layer; WM, white matter; FA, fractional anisotropy; SD-OCT, spectral domain optical coherence tomography; TBSS, tract-based spatial statistics; Fx, fornix; lCG, left cingulum cingulate gyrus.

between GC-IPL thickness and WM FA/MD in CIND or AD groups. However, trends were observed in the CIND and the AD groups if a lower threshold was used (TFCE uncorrected $p < 0.05$). In the CIND group, thinner GC-IPL was correlated with lower FA (and higher MD) in the fornix, CG, SLF, IFO, CST, and ATR (Fig. 2A, Supplementary Table 5). In the AD group, thinner GC-IPL was correlated with lower FA in the fornix, left CG, bilateral SLF, IFO, CST, and ATR (Fig. 2B, Supplementary Table 5). Conversely, FA or MD in the fornix was not correlated with the GC-IPL thickness for the NCI group even at this lower threshold of uncorrected $p < 0.05$.

In addition, we repeated the analyses on subjects across all three groups and found largely similar results as in NCI (FWE corrected $p < 0.05$) (Supplementary Table 4). The associations between WM and GC-IPL thickness in NCI were possibly driving the effects found in the analyses across all subjects. We also performed direct statistical comparisons of the WM-retina relationship between groups (see Supplementary Methods). Similar WM-retina relationship differences between NCI, CIND, and AD were observed (Supplementary Table 7). To ensure that the observed association was not confounded by antidepressants, anxiolytics, and/or antipsychotics medications, we performed the same retina-WM association analyses without participants who took these medications (1 NCI, 2 CIND, and 4 AD). Similar results were found (Supplementary Tables 9 and 10).

Thinner GC-IPL is related to lower GMV

Correlation between GC-IPL thickness and GMV was not significant at the threshold of FWE corrected $p < 0.05$ in any of the three groups or across all subjects. In NCI, a trend was observed in left calcarine gyrus, left lingual gyrus, and right cerebellum at the threshold of uncorrected $p < 0.001$ with minimum cluster size of 500 voxels (see Fig. 3 and Supplementary Table 6). No GMV-retina association was observed in the other two groups, even at the lower uncorrected threshold. Direct statistical comparisons of the GMV-retina relationship between groups (see Supplementary Methods) revealed

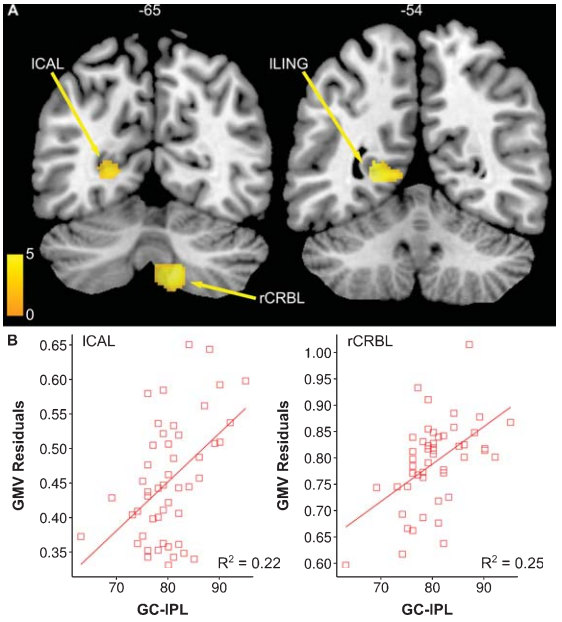

Fig. 3. Correlation of GC-IPL thickness with grey matter volume in the NCI group. A) Voxel-wise Linear Regression based on VBM revealed trend of positive correlation (uncorrected $p < 0.001$, cluster size >500 voxels) of GC-IPL thickness with GMV in brain regions highlighted in orange color. B) The subject-level mean GMV values from two clusters (pointed by the yellow arrows in A) in the NCI group were plotted against the GC-IPL thickness for the NCI (red squares and red line) after regressing out the effects of HD-OCT scanner signal strength, age, gender, handedness, and ethnicity. Adjusted R^2 was reported for each cluster. NCI, no cognitive impairment; GC-IPL, ganglion cell-inner plexiform layer; GMV, grey matter volume; FWE, family-wise error; SD-OCT, spectral domain optical coherence tomography; lCAL, left calcarine; lLING, left lingual; rCRBL, right cerebellum.

similar GMV-retina relationship differences in occipital regions and cerebellum (Supplementary Table 8).

DISCUSSION

Macular GC-IPL thinning was associated with lower WM microstructure integrity in NCI in frontal, parietal, occipital, and cingulum regions, as well as GMV reduction in occipital lobe and cerebellum. In contrast, such relationship was largely attenuated in AD and CIND; instead, weak relationship between GC-IPL thinning and WM loss in the fornix was hinted in both CIND and AD but not in NCI participants. As far as we know, our study is the first in the AD-related literature to demonstrate the WM-retina associations. Our findings suggested a disruption of age-related normal physiological retina-brain relationships due to disease-induced changes in patients with AD or early cognitive impairment.

Previous studies have demonstrated the effect of aging on brain WM microstructural disruption [36], GMV loss [36, 40, 41], and GC-IPL thinning [42] separately. One step further, we found both WM microstructure and GMV were associated with GC-IPL thickness in healthy older adults. One possible mechanism is the normal aging processes in both retina and brain structures. Individual difference in retina measures was associated with brain structure, suggesting that a strong link between retina and brain structural integrity in healthy aging. Nevertheless, the retina-brain associations exhibited regional heterogeneity in healthy aging.

Region-specific WM microstructure was related to the GC-IPL thickness in NCI. Compared to short-distance fiber, long-distance fibers, such as cingulum cingulated bundles, SLF, IFO [43], and CST [44], are more vulnerable to aging [45], possibly underlay cognitive decline in normal aging (see review [46]). Likewise, in our study, brain WM tracts correlated with GC-IPL thinning were also those long-distance ones affected more by normal aging. In parallel, a recent study has [24] reported that lower GMV in temporal and occipital lobes were associated with thinning in GC-IPL. Using whole-brain voxel-wise regression, we further revealed that lower GMV in lingual, calcarine, and cerebellum were associated with GC-IPL thinning in NCI, regions previously found to be associated with normal aging [36, 41, 47–51]. Taken together, our results indicated that individual differences in brain structures particularly vulnerable to normal aging could be reflected by the thickness of macular GC-IPL in healthy elderly. It further suggested that GC-IPL thinning might reflect degradation of brain structure in normal aging. Further developed, retina measures could potentially become a window to access normal aging in the brain.

While association between GC-IPL thickness and brain structure in NCI was dominated by the effect of normal aging, this retina-brain relationship was influenced by the disease in patients with AD or MCI. Consistent with previous findings [23], we found that macular GC-IPL was thinner in CIND compared to NCI. Lower GMV and lower WM microstructure integrity in AD and CIND also largely resembled previous findings [4–7, 52]. The retina-GMV relationship was lost in CIND and AD. Association between the GC-IPL thickness and WM microstructure in SLF, IFO, CST, ATR, and cingulum regions were largely attenuated in CIND and AD. We suspect that the weak or missing association between brain structure and the GC-IPL thickness might be

due to different rates of decline in brain structure and retina along the disease progression. Intriguingly, small trends of relationship were hinted between WM microstructure in regions such as fornix and the GC-IPL thickness in CIND and AD, which was not seen in NCI. Fornix is heavily undermined by AD [53]. Our results suggested that the retina-brain relationship in CIND and AD might be dominated by disease-induced changes.

A couple of limitations are noted in this study. Firstly, the correlations between the GC-IPL thickness and the brain WM microstructure in CIND and AD were not significant at the same threshold as the retina-WM association in NCI. They were seen only when we lowered the threshold to the TFCE uncorrected p-value of 0.05. These results should be viewed with cautious as it only served as a weak trend rather than a strong evidence of the correlations. It is worth noting, however, that the trend of association was observed in fornix for both the CIND and the AD groups but not for the NCI. Direct comparisons of the retina-brain relationship between the NCI and CIND groups also implicated a similar trend (Supplementary Figure 3 and Supplementary Table 7). Longitudinal study with larger patient sample should follow to confirm the disease mechanism behind these retina-brain relationship changes. Larger samples are also needed for the GC-IPL difference between AD and the other two groups [23]. Furthermore, our NCI and CIND participants were grouped based on the objective measurements of cognitive impairments. Future work is needed to systematically examine the impact of memory specific impairment, indicated by both objective memory impairment and subjective memory complaints, on retina brain relationship if any using larger samples. Moreover, we used TBSS to project FA to a group-level WM fiber skeleton. Although TBSS can partially reduce the misalignment of FA images in a WM voxel-based analysis [34], detection of WM changes near the boundary of WM and GM may be less accurate. Similarly, the observed gray matter volume differences derived from VBM might be confounded by inaccurate tissue segmentation or registration [54].

Conclusion

This study addressed the gap between the retina literature and brain structure research in normal aging and dementia patient populations. We found that individual differences in brain structures (both WM microstructure and GMV) in regions particularly vulnerable to normal aging could be reflected by the thickness of macular GC-IPL in healthy elderly. These normal physiological retina-brain relationships were disrupted in patients with AD or MCI, accompanied with a trend of possible disease-induced associations. This study may corroborate the normal anatomic relationship between WM and retinal ganglion cell changes, improve our understanding of the physiological variations, and aid in the differentiation between physiological and pathological structural changes related to AD.

ACKNOWLEDGMENTS

We would like to thank all subjects for their participation in this study. This work was supported by an NMRC Centre Grant (NMRC/CG/013/2013 and NMRC/CG/NUHS/2010 to CC), the Biomedical Research Council, Singapore (BMRC 04/1/36/372 to JZ), the National Medical Research Council, Singapore (NMRC/CBRG/0088/2015 to JZ), and Duke-NUS Graduate Medical School Signature Research Program funded by Ministry of Health, Singapore.

Authors' disclosures available online (http://j-alz.com/manuscript-disclosures/16-0067r3).

SUPPLEMENTARY MATERIAL

The supplementary material is available in the electronic version of this article: http://dx.doi.org/10.3233/JAD-160067.

REFERENCES

[1] Soininen HS, Partanen K, Pitkänen A, Vainio P, Hänninen T, Hallikainen M, Koivisto K, Riekkinen PJ (1994) Volumetric MRI analysis of the amygdala and the hippocampus in subjects with age-associated memory impairment: Correlation to visual and verbal memory. *Neurology* **44**, 1660-1668.

[2] Laakso MP, Soininen H, Partanen K, Helkala E-L, Hartikainen P, Vainio P, Hallikainen M, Hänninen T, Sr PJR (1995) Volumes of hippocampus, amygdala and frontal lobes in the MRI-based diagnosis of early Alzheimer's disease: Correlation with memory functions. *J Neural Transm Park Dis Dement Sect* **9**, 73-86.

[3] Giuliani NR, Calhoun VD, Pearlson GD, Francis A, Buchanan RW (2005) Voxel-based morphometry versus region of interest: A comparison of two methods for analyzing gray matter differences in schizophrenia. *Schizophr Res* **74**, 135-147.

[4] Ferreira LK, Diniz BS, Forlenza OV, Busatto GF, Zanetti MV (2011) Neurostructural predictors of Alzheimer's disease: A meta-analysis of VBM studies. *Neurobiol Aging* **32**, 1733-1741.

[5] Chételat G, Landeau B, Eustache F, Mézenge F, Viader F, de la Sayette V, Desgranges B, Baron J-C (2005) Using voxel-based morphometry to map the structural changes associated with rapid conversion in MCI: A longitudinal MRI study. *Neuroimage* **27**, 934-946.

[6] Whitwell JL, Shiung MM, Przybelski SA, Weigand SD, Knopman DS, Boeve BF, Petersen RC, Jack CR (2008) MRI patterns of atrophy associated with progression to AD in amnestic mild cognitive impairment. *Neurology* **70**, 512-520.

[7] Risacher SL, Saykin AJ, West JD, Shen L, Firpi HA, McDonald BC (2009) Baseline MRI predictors of conversion from MCI to probable AD in the ADNI cohort. *Curr Alzheimer Res* **6**, 347-361.

[8] Fjell AM, Walhovd KB (2010) Structural brain changes in aging: Courses, causes and cognitive consequences. *Rev Neurosci* **21**, 187-221.

[9] Sullivan EV, Pfefferbaum A (2006) Diffusion tensor imaging and aging. *Neurosci Biobehav Rev* **30**, 749-761.

[10] Bozzali M, Falini A, Franceschi M, Cercignani M, Zuffi M, Scotti G, Comi G, Filippi M (2002) White matter damage in Alzheimer's disease assessed *in vivo* using diffusion tensor magnetic resonance imaging. *J Neurol Neurosurg Psychiatry* **72**, 742-746.

[11] Bozzali M, Franceschi M, Falini A, Pontesilli S, Cercignani M, Magnani G, Scotti G, Comi G, Filippi M (2001) Quantification of tissue damage in AD using diffusion tensor and magnetization transfer MRI. *Neurology* **57**, 1135-1137.

[12] Fellgiebel A, Müller MJ, Wille P, Dellani PR, Scheurich A, Schmidt LG, Stoeter P (2005) Color-coded diffusion-tensor-imaging of posterior cingulate fiber tracts in mild cognitive impairment. *Neurobiol Aging* **26**, 1193-1198.

[13] Friese U, Meindl T, Herpertz SC, Reiser MF, Hampel H, Teipel SJ (2010) Diagnostic utility of novel MRI-based biomarkers for Alzheimer's disease: Diffusion tensor imaging and deformation-based morphometry. *J Alzheimers Dis* **20**, 477-490.

[14] Medina D, deToledo-Morrell L, Urresta F, Gabrieli JDE, Moseley M, Fleischman D, Bennett DA, Leurgans S, Turner DA, Stebbins GT (2006) White matter changes in mild cognitive impairment and AD: A diffusion tensor imaging study. *Neurobiol Aging* **27**, 663-672.

[15] Huang J, Friedland RP, Auchus AP (2007) Diffusion tensor imaging of normal-appearing white matter in mild cognitive impairment and early Alzheimer disease: Preliminary evidence of axonal degeneration in the temporal lobe. *AJNR Am J Neuroradiol* **28**, 1943-1948.

[16] Naggara O, Oppenheim C, Rieu D, Raoux N, Rodrigo S, Dalla Barba G, Meder J-F (2006) Diffusion tensor imaging in early Alzheimer's disease. *Psychiatry Res Neuroimaging* **146**, 243-249.

[17] Xie S, Xiao JX, Gong GL, Zang YF, Wang YH, Wu HK, Jiang XX (2006) Voxel-based detection of white matter abnormalities in mild Alzheimer disease. *Neurology* **66**, 1845-1849.

[18] Zhang Y, Schuff N, Jahng G-H, Bayne W, Mori S, Schad L, Mueller S, Du A-T, Kramer JH, Yaffe K, Chui H, Jagust WJ, Miller BL, Weiner MW (2007) Diffusion tensor imaging of cingulum fibers in mild cognitive impairment and Alzheimer disease. *Neurology* **68**, 13-19.

[19] Kalus P, Slotboom J, Gallinat J, Mahlberg R, Cattapan-Ludewig K, Wiest R, Nyffeler T, Buri C, Federspiel A, Kunz D, Schroth G, Kiefer C (2006) Examining the gateway to the limbic system with diffusion tensor imaging: The perforant pathway in dementia. *Neuroimage* **30**, 713-720.

[20] Sexton CE, Mackay CE, Lonie JA, Bastin ME, Terrière E, O'Carroll RE, Ebmeier KP (2010) MRI correlates of episodic memory in Alzheimer's disease, mild cognitive impairment, and healthy aging. *Psychiatry Res Neuroimaging* **184**, 57-62.

[21] Sexton CE, Kalu UG, Filippini N, Mackay CE, Ebmeier KP (2011) A meta-analysis of diffusion tensor imaging in mild cognitive impairment and Alzheimer's disease. *Neurobiol Aging* **32**, 2322.e5-2322.e18.

[22] Thomson KL, Yeo JM, Waddell B, Cameron JR, Pal S (2015) A systematic review and meta-analysis of retinal nerve fiber layer change in dementia, using optical coherence tomography. *Alzheimers Dement (Amst)* **1**, 136-143.

[23] Cheung CY-L, Ong YT, Hilal S, Ikram MK, Low S, Ong YL, Venketasubramanian N, Yap P, Seow D, Chen CLH, Wong TY (2015) Retinal ganglion cell analysis using high-definition optical coherence tomography in patients with mild cognitive impairment and Alzheimer's disease. *J Alzheimers Dis* **45**, 45-56.

[24] Ong Y-T, Hilal S, Cheung CY, Venketasubramanian N, Niessen WJ, Vrooman H, Anuar AR, Chew M, Chen C, Wong TY, Ikram MK (2015) Retinal neurodegeneration on optical coherence tomography and cerebral atrophy. *Neurosci Lett* **584**, 12-16.

[25] Hilal S, Chai YL, Ikram MK, Elangovan S, Yeow TB, Xin X, Chong JY, Venketasubramanian N, Richards AM, Chong JPC, Lai MKP, Chen C (2015) Markers of cardiac dysfunction in cognitive impairment and dementia. *Medicine (Baltimore)* **94**, e297.

[26] Hilal S, Ikram MK, Saini M, Tan CS, Catindig JA, Dong YH, Lim LBS, Ting EYS, Koo EH, Cheung CYL, Qiu A, Wong TY, Chen CL-H, Venketasubramanian N (2013) Prevalence of cognitive impairment in Chinese: Epidemiology of Dementia in Singapore study. *J Neurol Neurosurg Psychiatry* **84**, 686-692.

[27] Yeo DHH, Gabriel C, Chen C, Lee S, Loenneker T, Wong M (1997) Pilot validation of a customized neuropsychological battery in elderly Singaporeans. *Neurol J South East Asia* **2**, 1-8.

[28] Hilal S, Saini M, Tan CS, Catindig JA, Dong YH, Holandez RL, Niessen WJ, Vrooman HA, Ting E, Wong TY, Chen C, Venketasubramanian N, Ikram MK (2015) Intracranial stenosis, cerebrovascular diseases, and cognitive impairment in Chinese. *Alzheimer Dis Assoc Disord* **29**, 12-17.

[29] Wahlund LO, Barkhof F, Fazekas F, Bronge L, Augustin M, Sjögren M, Wallin A, Ader H, Leys D, Pantoni L, Pasquier F, Erkinjuntti T, Scheltens P, on behalf of the European Task Force on Age-Related White Matter Changes (2001) A new rating scale for age-related white matter changes applicable to MRI and CT. *Stroke* **32**, 1318-1322.

[30] Jenkinson M, Beckmann CF, Behrens TEJ, Woolrich MW, Smith SM (2012) FSL. *Neuroimage* **62**, 782-790.

[31] Cortese S, Imperati D, Zhou J, Proal E, Klein RG, Mannuzza S, Ramos-Olazagasti MA, Milham MP, Kelly C, Castellanos FX (2013) White matter alterations at 33-year follow-up in adults with childhood attention-deficit/hyperactivity disorder. *Biol Psychiatry* **74**, 591-598.

[32] Rueckert D, Sonoda LI, Hayes C, Hill DLG, Leach MO, Hawkes DJ (1999) Nonrigid registration using free-form deformations: Application to breast MR images. *IEEE Trans Med Imaging* **18**, 712-721.

[33] Van Dijk KRA, Sabuncu MR, Buckner RL (2012) The influence of head motion on intrinsic functional connectivity MRI. *Neuroimage* **59**, 431-438.

[34] Smith SM, Jenkinson M, Johansen-Berg H, Rueckert D, Nichols TE, Mackay CE, Watkins KE, Ciccarelli O, Cader MZ, Matthews PM, Behrens TEJ (2006) Tract-based spatial statistics: Voxelwise analysis of multi-subject diffusion data. *Neuroimage* **31**, 1487-1505.

[35] Andersson JLR, Jenkinson M, Smith S (2007) Non-linear optimisation. FMRIB technical report TR07JA1.

[36] Good CD, Johnsrude IS, Ashburner J, Henson RN, Friston KJ, Frackowiak RS (2001) A voxel-based morphometric study of ageing in 465 normal adult human brains. *Neuroimage* **14**, 21-36.

[37] Ashburner J (2007) A fast diffeomorphic image registration algorithm. *Neuroimage* **38**, 95-113.

[38] Smith SM, Nichols TE (2009) Threshold-free cluster enhancement: Addressing problems of smoothing, threshold dependence and localisation in cluster inference. *Neuroimage* **44**, 83-98.

[39] Hua K, Zhang J, Wakana S, Jiang H, Li X, Reich DS, Calabresi PA, Pekar JJ, van Zijl PCM, Mori S (2008) Tract probability maps in stereotaxic spaces: Analyses of white matter anatomy and tract-specific quantification. *Neuroimage* **39**, 336-347.

[40] Lim KO, Zipursky RB, Watts MC, Pfefferbaum A (1992) Decreased gray matter in normal aging: An *in vivo* magnetic resonance study. *J Gerontol* **47**, B26-B30.

[41] Raz N, Lindenberger U, Rodrigue KM, Kennedy KM, Head D, Williamson A, Dahle C, Gerstorf D, Acker JD (2005) Regional brain changes in aging healthy adults: General trends, individual differences and modifiers. *Cereb Cortex* **15**, 1676-1689.

[42] Mwanza J-C, Durbin MK, Budenz DL, Girkin CA, Leung CK, Liebmann JM, Peace JH, Werner JS, Wollstein G (2011) Profile and predictors of normal ganglion cell–inner plexiform layer thickness measured with frequency-domain optical coherence tomography. *Investig Opthalmology Vis Sci* **52**, 7872-7879.

[43] Sala S, Agosta F, Pagani E, Copetti M, Comi G, Filippi M (2012) Microstructural changes and atrophy in brain white matter tracts with aging. *Neurobiol Aging* **33**, 488-498.e2.

[44] Bastin ME, Maniega SM, Ferguson KJ, Brown LJ, Wardlaw JM, MacLullich AMJ, Clayden JD (2010) Quantifying the effects of normal ageing on white matter structure using unsupervised tract shape modelling. *Neuroimage* **51**, 1-10.

[45] Wu K, Taki Y, Sato K, Kinomura S, Goto R, Okada K, Kawashima R, He Y, Evans AC, Fukuda H (2012) Age-related changes in topological organization of structural brain networks in healthy individuals. *Hum Brain Mapp* **33**, 552-568.

[46] Bennett IJ, Madden DJ (2014) Disconnected aging: Cerebral white matter integrity and age-related differences in cognition. *Neuroscience* **276**, 187-205.

[47] Hafkemeijer A, Altmann-Schneider I, de Craen AJM, Slagboom PE, van der Grond J, Rombouts SARB (2014) Associations between age and gray matter volume in anatomical brain networks in middle-aged to older adults. *Aging Cell* **13**, 1068-1074.

[48] Douaud G, Groves AR, Tamnes CK, Westlye LT, Duff EP, Engvig A, Walhovd KB, James A, Gass A, Monsch AU, Matthews PM, Fjell AM, Smith SM, Johansen-Berg H (2014) A common brain network links development, aging, and vulnerability to disease. *Proc Natl Acad Sci U S A* **111**, 17648-17653.

[49] Bakkour A, Morris JC, Wolk DA, Dickerson BC (2013) The effects of aging and Alzheimer's disease on cerebral cortical anatomy: Specificity and differential relationships with cognition. *Neuroimage* **76**, 332-344.

[50] Raz N, Rodrigue KM (2006) Differential aging of the brain: Patterns, cognitive correlates and modifiers. *Neurosci Biobehav Rev* **30**, 730-748.

[51] Fjell AM, Westlye LT, Grydeland H, Amlien I, Espeseth T, Reinvang I, Raz N, Holland D, Dale AM, Walhovd KB (2013) Critical ages in the life course of the adult brain: Nonlinear subcortical aging. *Neurobiol Aging* **34**, 2239-2247.

[52] Alves GS, Knochel VO, Knnochel C, Carvalho AF, Pantel J, Engelhardt E, Laks J (2015) Integrating retrogenesis theory to Alzheimers disease pathology: Insight from DTI-TBSS investigation of the white matter microstructural integrity. *BioMed Res Int* **2015**, e291658.

[53] Nowrangi MA, Rosenberg PB (2015) The fornix in mild cognitive impairment and Alzheimer's disease. *Front Aging Neurosci* **7**, 1-7.

[54] Kennedy KM, Erickson KI, Rodrigue KM, Voss MW, Colcombe SJ, Kramer AF, Acker JD, Raz N (2009) Age-related differences in regional brain volumes: A comparison of optimized voxel-based morphometry to manual volumetry. *Neurobiol Aging* **30**, 1657-1676.